ZnO@porous media, their PL and laser effect

Bouvy, Claire; Su, Bao-Lian

Published in:
Journal of Materials Science & Technology

Publication date:
2008

Document Version
Early version, also known as pre-print

• *Key Invited Review*

ZnO@Porous Media, Their PL and Laser Effect

C.Bouvy and B.L.Su†
Laboratory of Inorganic Materials Chemistry, The University of Namur (FUNDP), 61 rue de Bruxelles, B-5000 Namur, Belgium

[Manuscript received December 17, 2007, in revised form February 19, 2008]

Claire Bouvy received her Master degree and PhD degree under the supervision of Prof. Dr. Bao-Lian Su from the Laboratory of Inorganic Materials Chemistry, University of Namur (FUNDP), Belgium, in 2003 and 2007, respectively. She carried out her researches on the optical properties and random lasing effect of ZnO nanoparticles confined inside the structure of micro- and mesoporous silica materials (thin films and powders). She is currently working in the Laboratory of Inorganic Materials Chemistry as a "Chargé de Recherche" in the frame of the Fonds National de Rechercher Scientifique (FNRS), Belgium.

Bao-Lian Su received his B.Sc. from University of Liaoning in 1983, and M.Sc. from Chengdu Institute of Organic Chemistry, Chinese Academy of Sciences in 1986. From September 1986 to September 1989, he held a research position at the Research Institute of Petroleum Processing, Beijing, China. He obtained his Ph.D. degree at Université P.M.Curie, Paris, France in 1992. He carried out his postdoctoral research in the Laboratory of Catalysis at the University of Namur (FUNDP), Belgium in 1993–1994. After holding a research position at Catalytica Inc. (Mountain View, California, USA), in September, 1995, he joined the faculty at the University of Namur and created the Laboratory of Inorganic Materials Chemistry (CMI). He is currently a Full Professor of Chemistry, Head of the Chemistry Department, Director of the Research Centre for Nanomaterials Chemistry and the Laboratory of Inorganic Materials Chemistry. Prof. Su received a series of honours and awards such as the Invention Award of Sinopec (1992) and A. Wetrems Prize of the Belgian Royal Academy of Sciences (2007). He is the President of Chemical Society and the President of Materials Research Society of Chinese Scholars in Belgium. He serves as the President of Namur Division of the Royal Chemical Society of Belgium since 2007. He has published more than 200 outstanding scientific papers and 3 patents. His papers have been cited more than 2000 times. His current research fields include the synthesis, the property study and the molecular engineering of organized, hierarchically porous and bio-inspired materials and nanostructures for nanotechnology, biotechnology, information technology and biomedical applications.

Optoelectronic nanocomposites are a new class of materials, which exhibit very interesting and particular properties and attract a growing attention due to their potential applications in information storage and optoelectronic devices. Zinc oxide, ZnO, is one of the most interesting binary semiconductor (3.37 eV) with very important optical properties, which can be used in the fields such as short wavelength lasers, blue light emitting diodes, UV detectors, gas sensors, *etc.* This paper reviews the very recent progress in the preparation of silica-based ZnO nanocomposites. After an introduction reviewing the theoretical background, the article will begin with a survey of the optical properties and the quantum size effect (QSE) of ZnO/SiO_2 nanocomposites prepared by the inclusion of ZnO nanoclusters inside silica mesoporous materials. The second part will focus on one of the most interesting properties of ZnO/SiO_2 nanocomposites, which is the random

† Prof., Ph.D., to whom correspondence should be addressed,
E-mail: bao-lian.su@fundp.ac.be.

lasing effect after one- and two-photon excitation. The final part will deal with the introduction of ZnO nanoparticles inside microporous zeolites and the observation of QSE. For comparison, the photoluminescence (PL) and QSE properties of ZnS nanoparticles occluded in mesoporous media are also described. New potential applications will be discussed since short-wavelength devices are required by industry to design, for instance, new information storage supports and biolabelling devices.

KEY WORDS: ZnO nanoparticles; Microporous and mesoporous materials; Quantum size effect; Random lasing effect

1. Introduction

From Democritus in ca. 400 BCE, who proposed the hypothesis that atoms possess unique properties such as size, shape and weight which are different from those of bulk materials (color and taste), to Feynman[1] who stated that "wires should be 10 or 100 atoms in diameter", Human has always been attracted by extremely small objects. The great challenge was how to explain what was happening at the atomic scale. Therefore, scientists have developed instruments and models which, finally, led to the observation and manipulation of atoms. At this scale, nanomaterials display exceptional properties, which can not be described by classical laws. The research area dealing with the study of these new properties is called nanoscience, and their utilizations towards potential new applications constitute the foundation of the field of nanotechnology.

Among all the original properties of nanomaterials, the most remarkable one is undoubtedly the quantum size effect (QSE)[2–7].

Bulky inorganic semiconductors have the ability to absorb and emit electromagnetic radiations ranging from UV to visible light. When semiconductors are composed of one (film), two (wire) or three nanometric dimensions (sphere), their optical, electrical or even photocatalytic properties are radically modified because the continuous valence and conduction bands become discrete levels. As a result, the bandgap between levels filled with electrons and levels unoccupied is increased. This is the so-called QSE. The broadening of the bandgap can be quantified and the basis of the explanation lies on the Schrödinger equation for one-dimensional time-independent systems[8,9]:

$$\frac{\mathrm{d}^2\Psi}{\mathrm{d}x^2} + \frac{2m}{\hbar^2}(E-U)\Psi = 0 \tag{1}$$

This wave equation, for a particle with a mass m moving in a potential U, gives the correct energy eigenvalues for the hydrogen-like atom. An electron in a nanometric semiconducting material can be regarded as the "particle in a box" model consisting in a single point particle enclosed in a box inside of which the potential is zero and at the walls of the box, the potential rises to infinity. The wave equation is becoming:

$$-\frac{\hbar^2}{2m}\frac{\mathrm{d}^2\Psi}{\mathrm{d}x^2} = E\Psi \tag{2}$$

This is a well studied differential equation and eigenvalue problem with a general solution of:

$$\Psi(x) = A\sin(kx) + B\cos(kx) \tag{3}$$

where A and B can be complex values, and k, the wavenumber, can be any real number. In order to find the specific solution for the problem, the appropriate boundary conditions must be specified:

$$\Psi(0) = 0 \text{ which implies that } \Psi(0) = B$$

$$\Psi(L) = 0 \text{ which implies that}$$

$$\Psi(L) = A\sin kL, \text{ with } A \neq 0$$

If $A \neq 0$, then $\sin(kL)=0$ only when $kL=n\pi$. The complete set of energy eigenfunctions for the one-dimensional particle in a box problem is then:

$$E_\mathrm{n} = \frac{n^2h^2}{8mL^2} \tag{4}$$

In a semiconductor material submitted to adequate electromagnetic radiation, one electron can be promoted from the fundamental energy level to the excited energy level. Simultaneously, one positive charge, called *hole*, is created and is in Coulomb interaction with the excited electron, which finally forms an *exciton*. This electrostatic interaction has to be taken into account in the energy expression of the excited semiconductor nanoparticle. In conclusion, the enhancement of the semiconductor bandgap (E^*) due to QSE is given by the energy of the bulky semiconductor (E_bulk), incremented by the confinement energy and the Coulomb interaction:

$$E^* = E_\mathrm{bulk} + \frac{h^2}{8\mu R^2} - \frac{1.8e^2}{4\pi\varepsilon_0\varepsilon_\infty R} \tag{5}$$

where μ is the effective mass of the exciton, ε_∞ the high-frequency dielectric constant and R the radius of the particle. The QSE is only significant for systems which possess dimensions of the order, or smaller than the Bohr radius of the exciton. Although a relation between the semiconductor dimensions (R) and the enhancement of the bandgap (E^*) is established, it is still difficult to obtain reliable sizes on the basis of experimental E^* since values for the effective masses and the optical dielectric constant were obtained for bulk materials.

Since last decades, some experimental evidences for QSE have been obtained for various IV, III-V and II-VI semiconductors[10,11]. For instance, a lot of work have been devoted to study the size-dependent luminescence of Si[12–14], which show significant blue-shift upon decreasing the size of the clusters due to the relatively large Bohr radius of Si (about 5 nm[15]). On the other hand, although their preparation is quite complex, InAs nanoparticles of different sizes have shown significant QSE[16,17], which can be of great importance since InAs can be used for the design of nanocrystal-based light-emitting diodes[18]. Finally, a lot of researches have been dedicated to the successful size tuning of CdSe nanoparticles and the observation

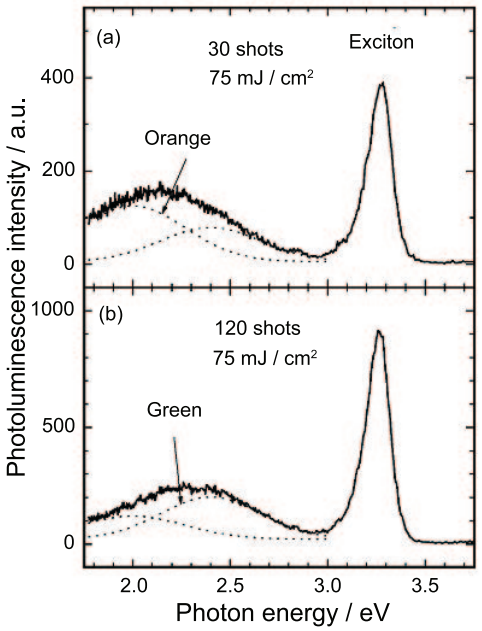

Fig.1 Room temperature photoluminescence spectra of ZnO nanocrystalline film annealed in ambient air at laser fluence of 75 mJ/cm^2: (a) 30 laser shots; (b) 120 laser shots. The dotted lines present the Gaussian fitting[47]

of the expected QSE[19−22]. The production of such nanocrystals opens a large variety of applications including biological labeling devices and light-emitting diodes. ZnO is also a II-VI semiconductor of great interest in the field of optics, electronics, (photo) catalysis, piezoelectric devices, gas sensors, *etc*[23−39].

ZnO is a wide direct bandgap semiconductor (3.37 eV[40]) with a high exciton binding energy (60 meV[41−43]), which makes exciton particularly stable even at high temperature (up to 550 K[44,45]) in comparison with other wide bandgap semiconductor (for instance, the exciton binding energy in ZnSe and GaN is only 22 and 25 meV, respectively). Upon appropriate excitation, the photoluminescence (PL) of ZnO is observed at 3.28 eV, which corresponds to the radiative recombination of excitons. Other PL bands can be observed in the orange and green region, at 2.0 and 2.4 eV, respectively[46,47] (Fig.1). Although a large number of studies have been devoted to the PL of ZnO, the origin of the visible emission can not unambiguously be explained. Egelhaaf and Oelkrug[48] reported that these defect-related luminescences are caused by radiative transitions between shallow donors (related to oxygen vacancies) and deep acceptors (Zn vacancies). The green band is assigned usually to PL of oxygen vacancies[49−51] (Fig.2), while the orange band is due to regions with local oxygen excess[52,53]. Another special feature of ZnO is its morphological variety[54−56] (Fig.3): nanorods[57], nanowires[24,58,59], nanobelts[60], nanocables[61], nanohelixes[62], hexagonal nanoplates[63], nanowire arrays[64], hierarchical nanostructures[65], hierarchically porous nanoparticles[66]. The growth mechanisms of such nanomaterials with various morphologies have been extensively investigated and some growth models have been proposed by Xu *et al.*[64] and others[59,63,64,66].

Concerning the preparation of ZnO nanomaterials, both physical and chemical methods can be considered. For instance, molecular beam epitaxy (MBE)[68−71], pulsed laser deposition (PLD), in controlled atmosphere[46,72,73] or in liquids[74−77], metal-organic chemical vapor deposition (MOCVD)[78−81] have been used to yield nanostructured thin films with high homogeneity, high crystallinity and adaptable chemical compositions. Aside from these "top-down" approaches, chemical methods, called "bottom-up" methods[59,63,64,66], are more valuable to grow ZnO particles to a specific size to obtain the expected QSE. Although the crystalline quality may be less good due to the potential presence of impurities in the solution phase, electrochemical[82,83], sol-gel[84,85] or even hydrothermal pathways[86−90] are known to lead to extremely small particles with tunable dimensions. During the particle growth in these homogeneous solutions, it is essential to arrest growth when the required particle size is obtained. The conventional strategy implies the preparation of ZnO inside the hydrophilic core of reverse micelles in non-polar solutions[91] or the addition of capping agents[92], which limit the size of the growing particle. An alternative approach, on which we will focus in this review, is the synthesis of particles inside polymeric matrixes[93−96] or porous structures whose channels are able to restrict diameters to determined dimensions. It is important to choose porous materials with controlled porosity, which can guarantee a good dispersion of particles and avoid their aggregation, and also porous materials, which can be easily handled considering optical or electronic applications.

2. ZnO Inside Mesoporous Silicas: Preparation and Optical Properties

2.1 Overview

Micro-[97] and mesoporous silica materials[98,99] are ideal candidates[100] for the encapsulation of semiconducting nanoparticles. Indeed, high surface area, pore diameter ranging from less than 2.0 nm (microporous materials, *i.e.* zeolites) up to 50.0 nm (mesoporous materials), well-organized channels, internal

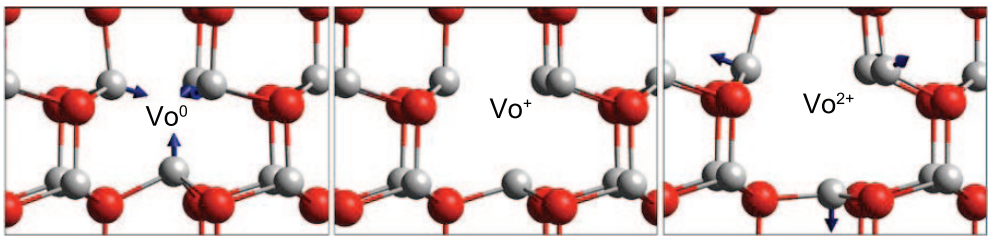

Fig.2 Ball and stick representation of the local atomic relaxations around the oxygen vacancy in the 0, 1+, and 2+ charge states[51]

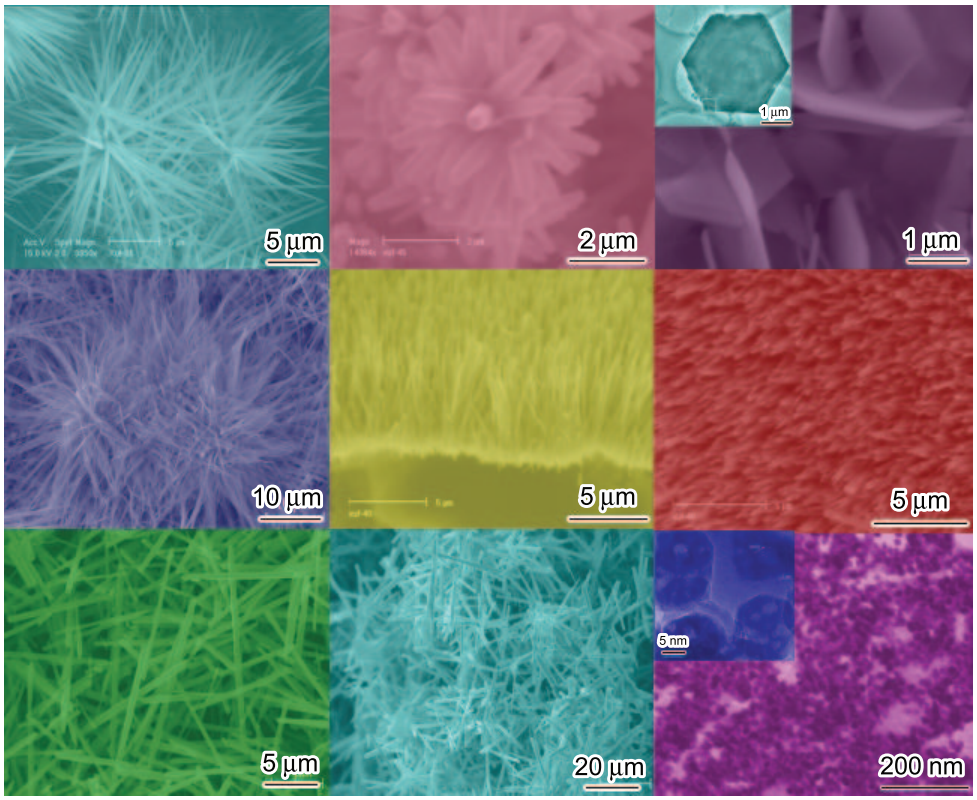

Fig.3 Collection of nanostructures of ZnO by hydrothermal synthesis from literature [24,59,63,64,66]

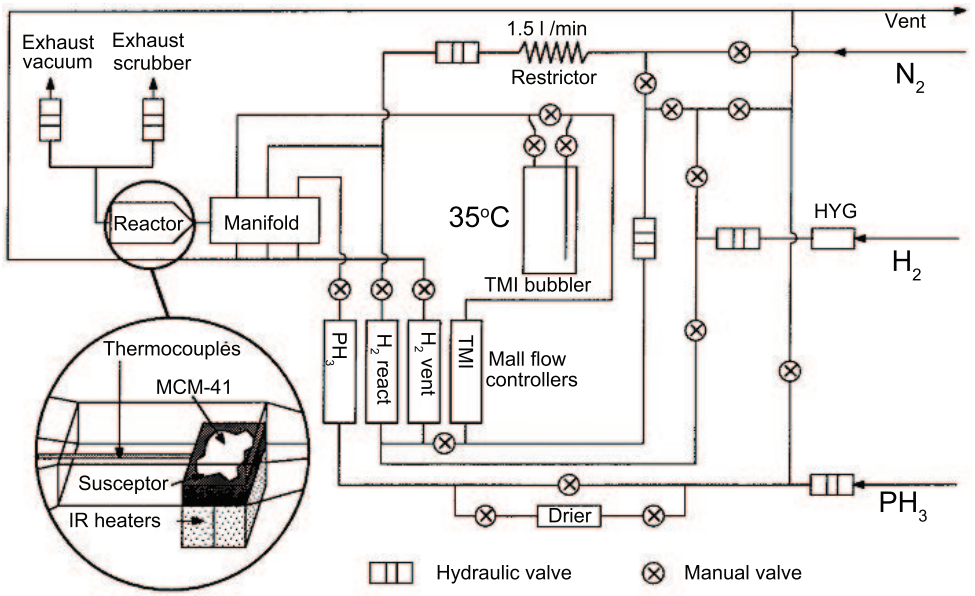

Fig.4 Simplified plan of the MOCVD reactor, showing gas inlets, gas mass flow controllers, reactor manifold, and glass reactor[112]

reactive silanols (Si–OH) groups and good mechanical, thermal and hydrothermal stability are their undeniable advantages. The synthesis of mesoporous materials implies the preparation of a micellar aqueous solution followed by the addition of an inorganic silica source, which will hydrolyze and condensate around the cylindrical micelles in order to form a dense silica network after surfactant removal[101−105]. According to the nature of the surfactant and the silica source, materials with different characteristics can be obtained: MCM-41[98,99], SBA-15[106], MSU[107] or even CMI-1[108]. While zeolites, a familiy of crystalline microporous materials, are formed by the condensation of silica and alumina sources in aqueous solutions and the porosity is induced by single molecules or solvated cations, which act as structure directing agent. Various applications of zeolites and silica mesoporous materials have been reviewed by Corma in 1997[109]. Among them, a large attention was paid to optical applications[110]. MOCVD technique has been employed to grow nanoparticles of GaAs[111] and InP[112] inside the mesopores of MCM-41 siliceous material. An amount of mesoporous materials was loaded in the MOCVD reactor and heated at relatively high temperature (400–600°C) (Fig.4). For GaAs, tert-butylarsine and trimethylgallium, and

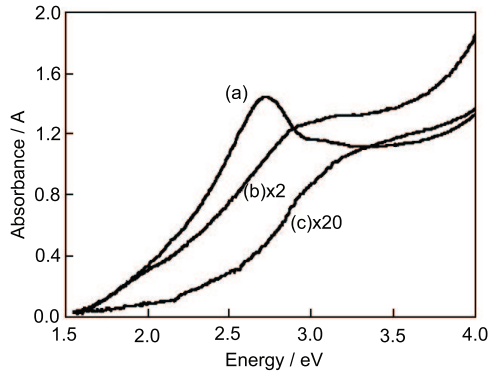

Fig.5 Absorption spectra of GaAs deposited on a fused silica substrate for different time deposition: for 250 s (a), on MCM-41 for 250 s (b) and on MCM-41 for 100 s (c)[111]

for InP, phosphine and trimethylindium, were used as metal-organic precursors. Based on optical measurements (Fig.5), the authors claimed that nanoparticles were grown inside the channels of MCM-41 and that QSE resulting in a blue-shift of the corresponding emission spectra was exhibited.

II-VI semiconductors are easier to introduce inside porous materials and do not require complex setup such as in MOCVD reaction. Their growth has been extensively investigated inside mesoporous silicas as well as inside zeolites. Different approaches have been considered and there are many synthesis methods as much as number of researchers′ teams working in the field. For instance, for CdS, the most common pathway consists of chemical modification of the internal surfaces of mesoporous silicas with either thiol[113−115] (Fig.6) or phenyl groups[116] followed by the impregnation of the functionalized material inside Cd^{2+} solutions. After subsequent thermal treatment under H_2S or N_2, CdS nanoparticles are formed inside the mesopores of MCM-41 and SBA-15. UV-Vis and PL spectra confirm the expected blue-shift arising from QSE, and the particle size can be estimated to be in the range of 1.0–2.0 nm (Fig.7). Instead of being formed after impregnation and calcination, CdS nanoparticles can also be prepared inside reverse micelles of sodium bis(2-ethylhexyl)sulfosuccinate (NaAOT) in water/isooctane solution by the reaction of $Cd(NO_3)_2$ with Na_2S[117]. In the same way, ZnS and Mn-doped ZnS nanoparticles were prepared successfully inside the channels of MCM-41, SBA-15 and CMI-1 mesoporous silicas. Significant blue-shift were observed and attributed to the size-quantified particles[118−120].

As explained at the beginning of this review, ZnO is a II-VI semiconductor, which attracts a lot of enthusiasm regarding the potential applications in so many fields. Due to the large interest of ZnO, both chemical and physical journals have dedicated publications to the ZnO/mesoporous silicas nanocomposites and the most significant studies will be reviewed in the following section with a particular attention given to the optical results.

The first research dealts with the preparation of sol-gel ZnO/SiO_2 nanocomposites. In most cases, an alcoholic solution of tetraethoxysilane (TEOS) was mixed with a solution of zinc nitrate or acetate and the sol obtained was allowed to gel during different times and eventually annealed in air or O_2 atmosphere. After reviewing the sol-gel method, the impregnation inside pure and functionalized mesoporous silicas will be discussed. Finally, alternative methods to load ZnO inside SiO_2 matrix will be mentioned.

2.2 Incorporation into disordered porous media: the sol-gel method

Cannas *et al.*[121] reported the synthesis of ZnO/SiO_2 nanocomposites by means of mixing ethanolic solution of TEOS with an aqueous solution of $Zn(NO_3)_2$. The sol was then aged at 90°C for one week and heated up to 900°C. High-angles X-ray diffraction (XRD) patterns reveal a broad band in the range 2θ: 20°–40° corresponding to amorphous silica. Upon heating the nanocomposites, two broadened features appeared and were attributed to ZnO nanoparticles. Further heating at 900°C led to a well-resolved XRD pattern ascribed to crystalline β-Zn_2SiO_4[122] emerging, according to the authors, from the creation of Zn–O–Si bonds. Additional confirmation was brought by ^{29}Si MAS NMR measurements, which indicates the effective presence of Zn–O–Si bonds inside the ZnO/SiO_2 nanocomposites.

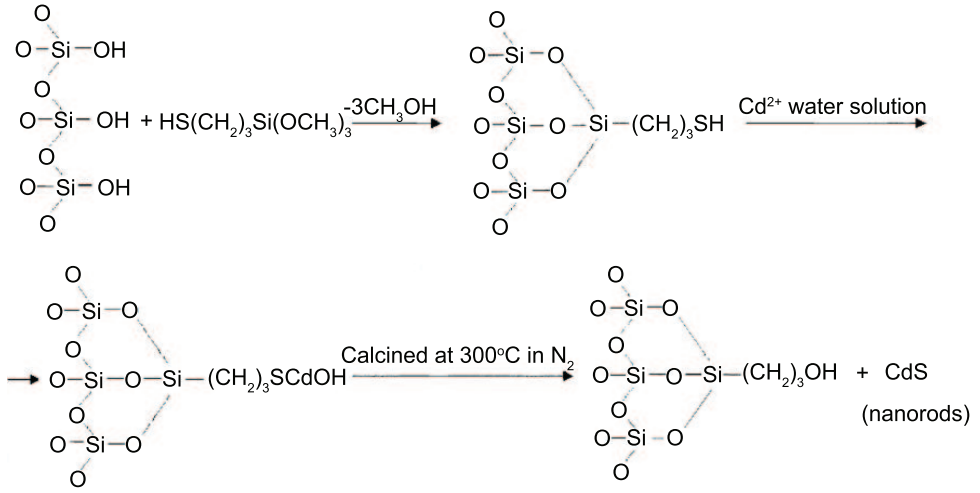

Fig.6 Simple *in situ* adsorption method combining a thiol group surface modification scheme and a wet impregnation method to synthesize mono-dispersive binary semiconductor CdS nanocrystals with uniform size inside the channels of mesoporous silicas[114]

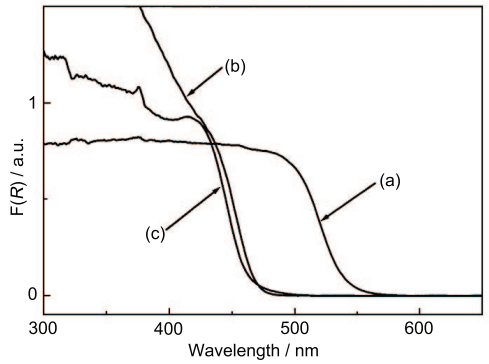

Fig.7 Diffuse reflectance UV-Vis spectra of CdS in various environments: (a) bulk CdS, (b) CdS/SBA-15, and (c) CdS/MCM-41[115]

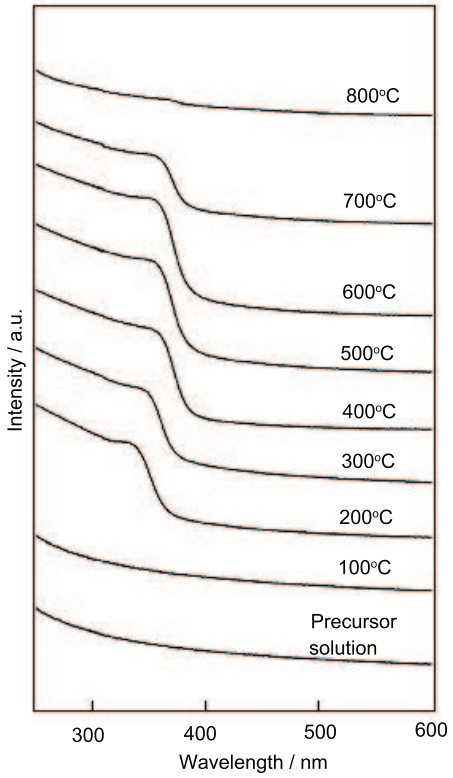

Fig.8 Evolution of the UV-Vis optical absorption spectra as a temperature function for precursor solution and for pure ZnO coatings[123]

Instead of using $Zn(NO_3)_2$ as the Zn precursor, zinc acetate was currently employed in the preparation of ZnO-based nanocomposite. Mixing ethanolic solution of TEOS with an ethanolic solution of $Zn(CH_3COO)_2$, sol-gel ZnO-based nanomaterials were obtained, which were subsequently dip-coated on silica substrates[123]. For annealing temperatures below 300°C, no XRD peaks were detected, which probably means that ZnO nanoparticles are not large enough to give diffraction signals. Relying on UV-Vis optical absorption spectra, the authors claimed that, at low annealing temperatures, the absorption onset was blue-shifted compared to bulk ZnO, which confirmed the presence of small ZnO nanoparticles inside the silica matrix and the presence of QSE (Fig.8).

The PL properties of sol-gel ZnO/SiO_2 nanocomposites were deeply investigated by the group of Chakrabarti and Wang in 2003[124−126]. They both observed defects bands of ZnO in the visible range and tried to determine their origin. Meanwhile, the UV peak related to the radiative recombination of excitons in ZnO was detected but was in only one case (Chakrabarti) blue-shifted to higher energies (4.2 eV) comparing to bulk ZnO because of the QSE. The authors developed a very good summary of the particle size determination based on the effective mass approximation and were able to estimate the ZnO particle dimensions to ca. 1.4–1.5 nm.

Another approach in the sol-gel method consisted in mixing together a silica sol and ZnO colloids formed by putting metallic zinc into hydrogen peroxide (H_2O_2) solution[127]. This process led to a silica gel containing $Zn(OH)_2$ species, which was finally aged and heated at 250°C. The influence of pH values of the sols, gelation temperatures and heating temperatures on optical properties was investigated by PL spectroscopy. In all spectra, a broad band peaked at 395 nm was observed and ascribed to the near band edge emission of bulk ZnO.

In summary, the sol-gel method successfully leads to ZnO/SiO_2 nanocomposites through very simple pathways, which implies the preparation of silica and ZnO sols and the subsequent mixing of these two solutions to form the final product after ageing and heating. However, QSE was not systematically observed because of the heterogeneity of the samples. Indeed, during the sol-gel process, no control on the porosity is allowed and, as a result, the particle size of ZnO can not be limited efficiently. Therefore, it became essential to use adequate hosts with well-defined porosity to grow ZnO particles and to produce QSE.

2.3 Inclusion in highly ordered mesoporous MCM-41 materials by impregnation

One of the first report dedicated to the introduction of ZnO nanoparticles inside the channels of silica mesoporous materials was made by Zhang *et al*. in 2000[128]. They described the conventional preparation of MCM-41 mesoporous materials followed by the functionalization of the internal surfaces with *N*-[3(trimethoxysilyl)-propylethylene] diamine molecules (designed TPED), which are able to chelate Zn^{2+} ions. After calcination in air atmosphere at 600°C to remove the organic molecules, ZnO/MCM-41 nanocomposites were obtained and intensively characterized. As already observed in some nanocomposites designed by the sol-gel method, no diffraction signals of crystalline ZnO were detected in the XRD pattern of ZnO/MCM-41 sample, which is, according to the authors, an indication of the good dispersion of ZnO inside the silica matrix. Furthermore, no ZnO particles have been discerned by transmission electron microscopy (TEM) probably because of the lack of contrast between ZnO and the SiO_2 network. Nevertheless, thanks to EDS analysis, the presence of ZnO nanoparticles inside the channels of MCM-41 was confirmed. By UV-Vis reflectance (Fig.9), the onset of absorption of ZnO/MCM-41 nanocomposite at 290 nm appeared to be blue-shifted in comparison to bulk ZnO (370 nm) because of the QSE of ZnO nanoparticles estimated to be smaller than 1.8 nm. The broad PL band corresponding to defects of ZnO was observed in the visible region of

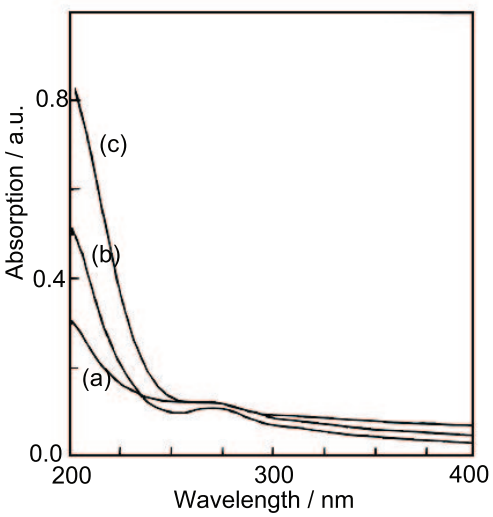

Fig.9 Diffuse-reflectance UV-vis spectra of samples with different ZnO contents: (a) ZnO-MCM-41 (0.002 mol/L), (b) ZnO-MCM-41 (0.01 mol/L), and (c) ZnO-MCM-41 (0.05 mol/L)[128]

the spectra and was also shifted to shorter wavelenghts due to confinement effect.

The same trends were reported later with MCM-41 modified with a silane-coupling agent, triethyoxyl-γ-ethyldiaminopropylsilane (designed TEEDPS)[129]. Although ZnO particles were not directly revealed by XRD and TEM, EDS analysis under high-resolution TEM showed signal representative of Zn species. According to the relation between the particle size and the wavelength of absorption onset given by UV-Vis absorption spectroscopy, the authors were able to estimate the ZnO dimensions to be around 1.7 nm, which is in good accordance with the previous communication. The UV PL band corresponding to the excitonic emission of ZnO was found at 377 nm in PL spectra, confirming the QSE deduced from UV-Vis measurements.

It was also demonstrated that the functionalization step with chelating organic molecules was not necessary to grow efficiently ZnO nanoparticles inside the channels of mesoporous silicas. For instance, ZnO/SiO_2 nanocomposites were prepared by impregnating commercial SiO_2 (average porosity=15 nm) with aqueous or ethanolic solutions of concentrated $Zn(NO_3)_2$[130]. XRD pattern reveals crystalline peaks upon the amorphous fingerprint of silica. When annealing up to 900°C, the crystalline phase β-Zn_2SiO_4 can be distinguished as already reported but no PL results are displayed. Instead of weak porous commercial silica, mesoporous MCM-41 was employed and soaked in solutions of zinc nitrate and/or acetate, and finally calcined under air or O_2 atmosphere. Again, no diffraction signal of crystalline ZnO was present in the XRD pattern of ZnO/MCM-41 nanocomposites, which is interpreted as a good dispersion of nanoparticles inside the silica network. The expected QSE was evidenced by PL[131], PL excitation[132] and diffuse-reflectance UV-Vis spectroscopies[133]. In most cases, even though the excitonic peak was not present in PL spectra, the band related to defects was always observed and blue-shifted towards shorter wavelengths.

The same results were obtained for ZnO/MCM-41 nanocomposites synthesized with zinc acetylacetonate

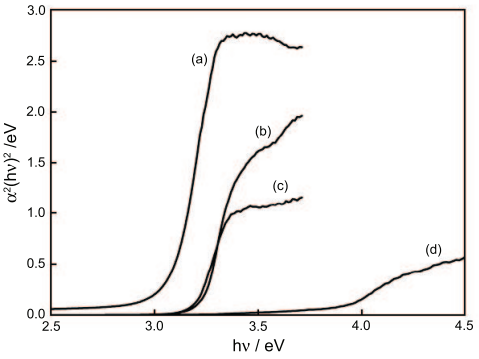

Fig.10 UV-Vis spectra of: (a) bulk ZnO, (b) mesoporous silica soaked in ethanolic $Zn(acac)_2$ solution with stirring, (c) mesoporous silica soaked in toluene $Zn(acac)_2$ solution with stirring, (d) mesoporous silica soaked in ethanolic $Zn(acac)_2$ solution without stirring[134]

($Zn(acac)_2$) as Zn precursor[134]. In this study, the authors present XRD patterns with diffraction peaks labeled to ZnO with wurtzite structure. Thanks to UV-Vis absorbance spectra, the particle size of ZnO in different nanocomposites was determined to be in the range 5–35 nm and QSE was produced by the smallest ZnO particles (Fig.10).

2.4 Inclusion in highly ordered mesoporous CMI-1 materials by impregnation

CMI-1 mesoporous materials[108] were also infiltrated with zinc nitrate solutions to lead to ZnO/CMI-1 nanocomposites. In order to highlight QSE in ZnO nanoparticle, the PL of the mesoporous matrix was first studied with an excitation source of 254 nm (photon energy of 4.88 eV). The corresponding PL spectrum was composed of two wide PL bands centred at 2.94 and 3.89 eV which are generated by the same defects associated with silanol groups[135]. For ZnO/CMI-1 nanocomposites, the PL spectroscopy gives a very wide PL band in the range 3.2–3.4 eV, in which the contribution of the ZnO nanoparticles and the mesoporous matrix have to be distinguished[136]. By a Gaussian decomposition, the PL band corresponding to ZnO has been revealed at 3.41 eV, which is shifted to higher energies compared with that of bulk ZnO (Fig.11). The shift was related to QSE from extremely small ZnO nanoparticles confined inside the channels of the mesoporous material CMI-1.

ZnS/CMI-1 nanocomposites were also prepared in the channels of ED-modified CMI-1 mesoporous materials and their photoluminescent properties have been studied[118]. Characterization results have confirmed the presence of ZnS inside the CMI-1 material and the PL spectrum of the ZnS/CMI-1 nanocomposite has shown an excitonic emission from bulk ZnS (3.25 eV) while an important blue-shifted emission attributed to QSE of extremely small ZnS nanoparticles was meanwhile revealed at 3.9 eV (Figs.12 and 13).

Recently, also based on the impregnation approach, a new series of optoelectronic composites with a highly organized mesoporous silica core and a uniform ZnS shell (200 nm in thickness) with new optical properties was reported[137]. The starting CMI-1

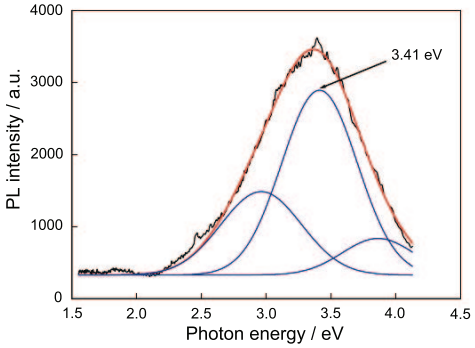

Fig.11 Photoluminescence spectrum (λ=254 nm) of sample ZnO/CMI-1 prepared by direct impregnation with its Gaussian decomposition[136]

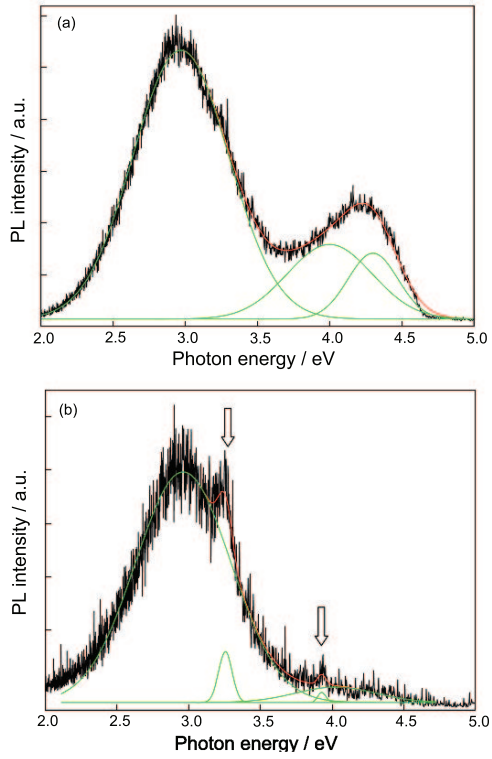

Fig.12 PL spectra of the ED-CMI-1 modified material (a) and the ZnS/ED-CMI-1 nanocomposite (b) (excitation=193 nm, 6.4 eV)[118]

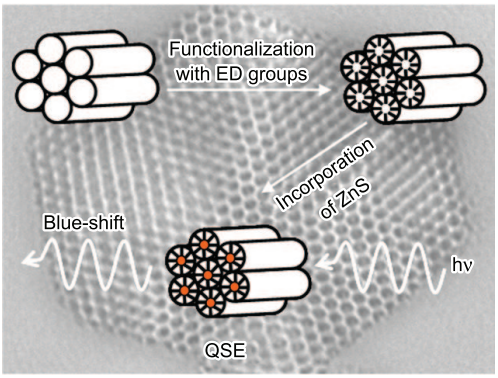

Fig.13 Scheme depicting the preparation of ZnS nanoparticles inside ED-modified CMI-1 mesoporous materials and the observation of quantum size effect[118]

material was firstly functionalized with ethylenediamine groups and then the growth of the ZnS shell was targeted by the immersion of the functionalized CMI-1 material in a $Zn(CH_3COO)_2$ solution followed by a reaction with sodium sulfide. For each particle, a homogeneous zinc sulfide shell with 200 nm in thickness surrounding a mesoporous silica core was observed by TEM (Fig.14). By PL spectroscopy, no band shift to high energy can be observed, suggesting that due to the formation of a ZnS shell, ZnS nanoparticles formed initially are gathered together to form larger aggregates with too large size to generate QSE (Fig.15).

2.5 Inclusion by alternative methods

Other alternative ZnO loading methods have been developed but, due to their relatively complex requirement, their application was limited to a few research groups. One can cite the spray-drying process, the electrochemical and the reverse micelles methods. The first one implies the preparation of a ZnO colloid solution[84] and its mixing with a SiO_2 colloid solution supplied commercially or synthesized from TEOS. The homogeneous mixture is then spray-dried in a vertical reactor, equipped with temperature adjustable heating zones, to produce micrometer/submicrometer-sized ZnO/SiO_2 powder composite[138,139]. Although QSE was not unambiguously demonstrated, the PL properties of these nanocomposites appeared to be remarkably stable with time, even after being aged over 30 d (Fig.16). The second approach implies the preliminary synthesis of SiO_2 thin films onto conductive glassy substrates[140,141]. These films were used as cathodes and dipped into an aqueous zinc chloride, $ZnCl_2$, solution for direct electrodeposition of ZnO. The authors measured the PL of bulk ZnO and of ZnO/SiO_2 nanocomposite at 384 and 369 nm, respectively (Fig.17). A significant shift towards shorter wavelengths was obviously detected and ascribed to nanometric ZnO particles grown inside the mesochannels of the SiO_2 thin film. Asides from the optical properties, the photoelectric properties of such nanocomposites were also investigated and an increased photoconductivity from the free electrons of ZnO was observed.

2.6 Inclusion by the reverse micelles method

The last method described in this section is somewhat different from the previous ones[142,143]. The ZnO particles are prepared by dissolving zinc acetate and NaOH in separate NaAOT reverse micelles solutions. Both systems are then mixed together and ZnO particles are formed inside the hydrophilic cores of micelles. After being stabilized by organic agents, the reverse micelles mixture was poured in tetramethoxysilane, TMOS, which hydrolyses and condensates leading to the formation of a silica network around the micelles. A calcination step allows the organic components to be removed and the ZnO/SiO_2 nanocomposite is finally obtained, as illustrated in Fig.18. Although the excitonic emission of ZnO was not directly observed, QSE can be deduced from the significant blue-shift of the defect luminescence band[142] or the ZnO emission band given by Gaussian decomposition of the PL spectrum[143] (Fig.19(a)). These results indicate that the reverse micelles method is a powerful approach to grow ZnO nanoparticles inside silica matrix with well-defined dimensions in the nanometric

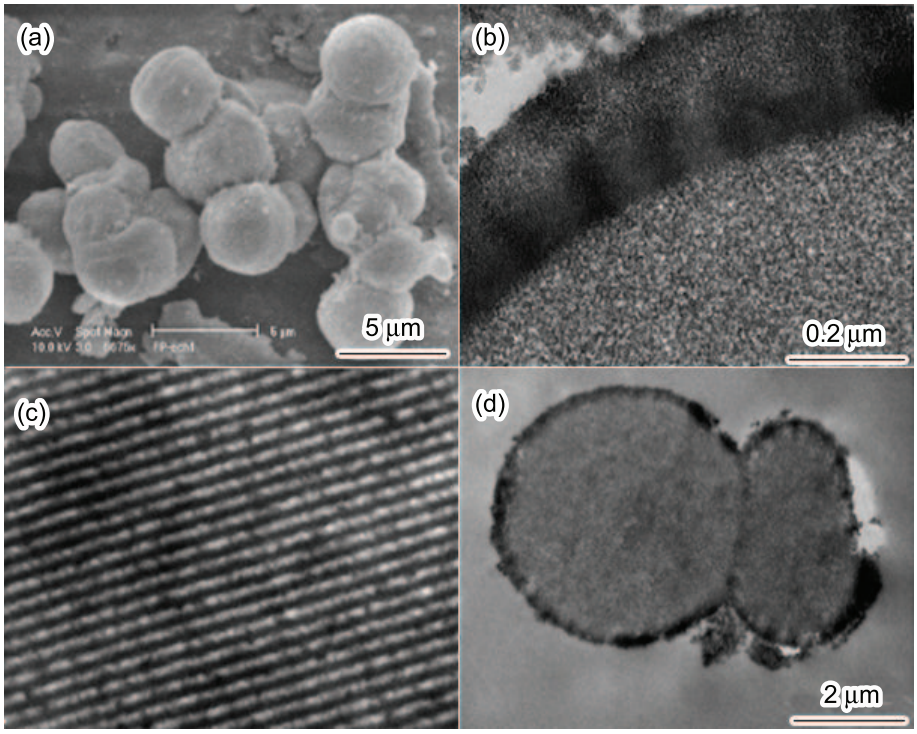

Fig.14 SEM micrograph (a) and TEM micrographs (b–d) of CMI-1/ZnS core/shell composite[137]

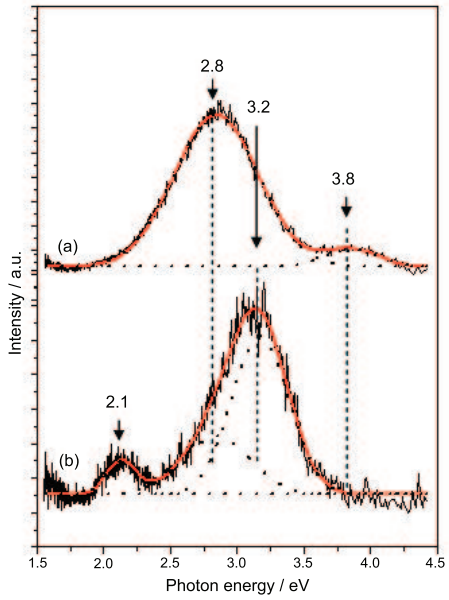

Fig.15 Photoluminescence spectra of: (a) CMI-1 material and (b) CMI-1/ZnS core/shell composite[137]

range.

3. ZnO inside Mesoporous Silicas: Random Laser Action

3.1 Random laser mechanism

All the methods reviewed up to now have successfully led to the introduction of small ZnO nanoparticles inside the network of mesoporous silica materials. Intensive characterizations have been carried out to determine structural, morphological, textural and optical properties. Unfortunately, no attention was paid to one of the most interesting and important properties of ZnO, which is the random lasing effect[144−151] predicted theoretically by Letokhov in 1967[152]

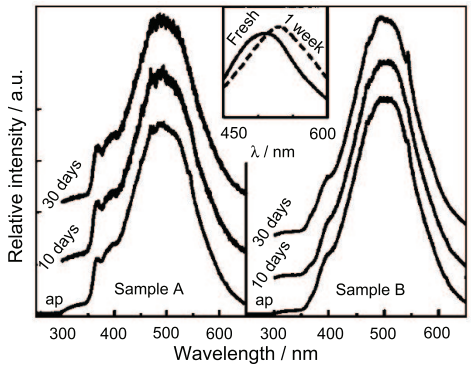

Fig.16 Dependence of PL spectra of samples A and B on aged period: as-prepared powders (ap), aged over 10 d, and aged over 30 d. Inset is the PL spectra of the ZnO colloid (0.1 mol/L); solid line: fresh colloid and dashed line: 1 week aged colloid[138]

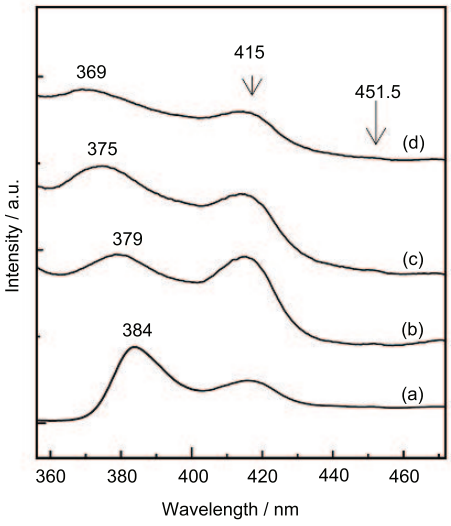

Fig.17 PL spectra from bulk ZnO (a), ZnO pillars (b), overgrown ZnO-MPS (c), and nanosized ZnO inside MPS films (d)[140]

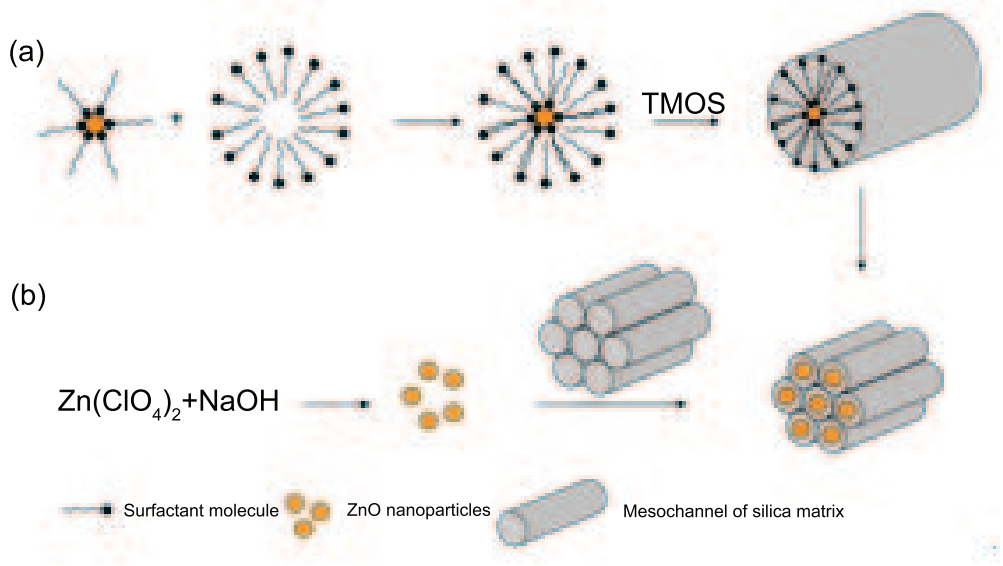

Fig.18 Scheme depicting the preparation of nanocomposites by the reverse micelles method (a) and the colloidal method (b)[143]

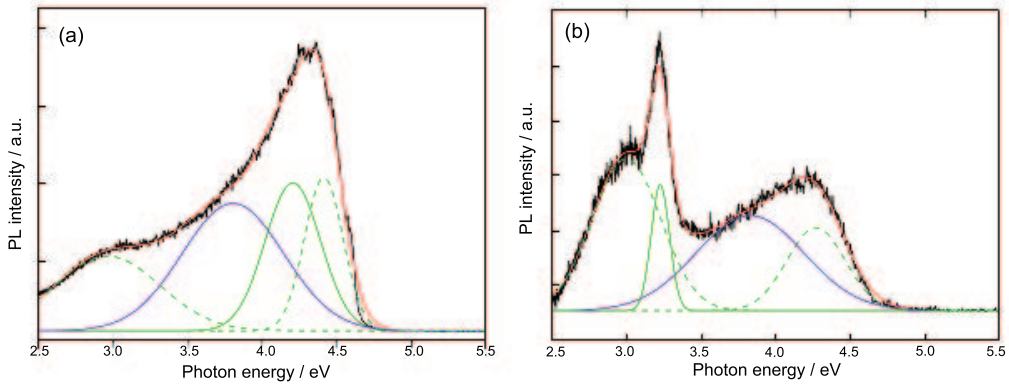

Fig.19 PL spectrum of ZnO/mesoporous silica nanocomposite prepared by the reverse micelle method (a) and the colloidal method (b) (excitation wavelength=193 nm)[143]

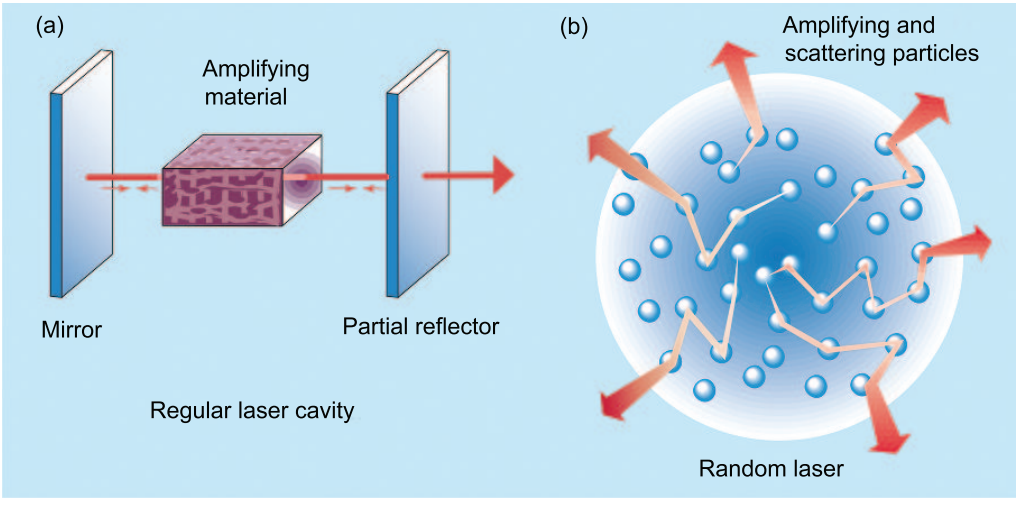

Fig.20 Comparison between a regular laser and a 'random laser': (a) in a regular laser the light bounces back and forth between two mirrors that form a cavity. After several passes through the amplifying material in the cavity, the gain amplification can be large enough to produce laser light; (b) in a random laser the cavity is absent but multiple scattering between particles in the disordered material keeps the light trapped long enough for the amplification to become efficient, and for laser light to emerge in random directions[144]

(Fig.20). ZnO nanofilms or nanoparticles can be considered as disordered materials, which act as strong scattering media for light waves. When an incident beam is sent on ZnO samples, the light will be diffused by the particles and its direction of propagation will be changed in an arbitrary way. If the scat-

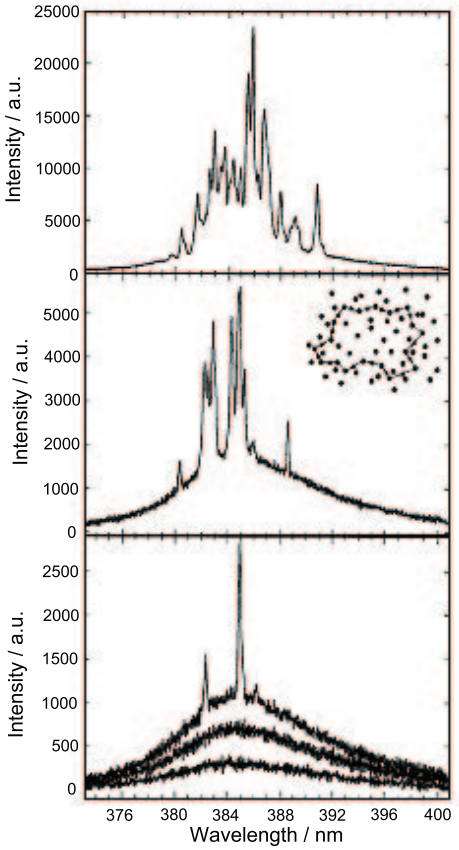

Fig.21 Spectra of emission from ZnO powder when the excitation intensity is (from bottom to top) 400, 562, 763, 875, and 1387 kW/cm^2. The inset is a schematic diagram showing the formation of a closed loop path for light through recurrent scattering in the powder[146]

tering mean free path becomes equal to or less than the incident wavelength, the wave light can return to a particle from which it was scattered before and eventually can form closed loop paths. The multiple scattering, which takes place in such disordered materials, can not really provide the feedback mechanism required for laser action, but it makes the light stay inside long enough to finally obtain efficient amplification. The scattering medium, which allows light to be amplified, is one of the conditions to make a laser. The other condition is to provide a feedback mechanism so that the light can be trapped in order for the amplification to be efficient. Since no real cavity guaranteeing the feedback of the light, the existence of laser action in ZnO disordered powders is a result of equilibrium between gain and loss. The gain is a function of the time spent by the light inside the amplifying material while the loss depends on the possibility for the light to escape from the material. If laser action occurs, it is because the gain becomes larger than the loss and this represents the threshold condition for the production of the laser effect. At incident excitation intensities below the threshold, the observed emission in spectra is due to the radiative recombination of ZnO. Above the intensity threshold, the peak grows rapidly to a much narrower signal corresponding to stimulated emission (Fig.21). If the excitation intensity is further increased, the emission turns broadened because

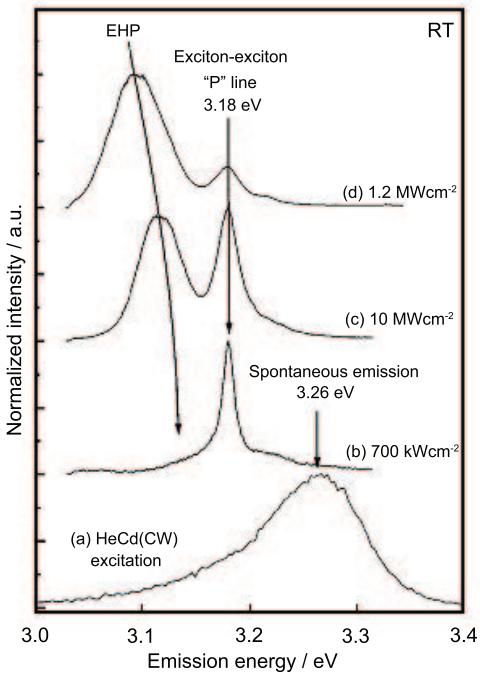

Fig.22 Normalized PL spectra of ZnO epitaxial layers for various excitation intensities at room temperature[44]

of the electron-hole plasma radiative recombination mechanism[153,154].

3.2 Random laser action in ZnO *films*

One of the first reports of lasing in ZnO was made in 1996 by Reynolds *et al.*[155], which used a HeCd laser to pump ZnO grown in platelets form. They demonstrated optically pumped lasing in ZnO at a very low pump power and observed well-defined lasing modes. Afterwards, other research groups have performed numerous studies dealing with the lasing of different ZnO samples and their work will be briefly summarized in the following section.

The group of Bagnall *et al.* has prepared ZnO epitaxial layers by plasma-assisted molecular beam epitaxy (MBE) and observed significant stimulated emission and lasing at room temperature with threshold intensities around 250 kW/cm^2 using the frequency-tripled output (355 nm) of a Nd:YAG laser (10 Hz, 6 ns)[44,45,156] (Fig.22). ZnO thin films were also grown on sapphire substrates by laser-MBE and their optical properties as well as their laser effect were studied at various pumping intensities of frequency-tripled output (355 nm) of a Nd:YAG laser[66,157−161]. The observed threshold for the transition between spontaneous emission of ZnO to stimulated emission was estimated to be 24 kW/cm^2, which is ten times less than the previous values reported.

3.3 Two-photon random laser action in ZnO*/CMI-1 nanocomposites*

Moreover, laser action in ZnO can also be produced after a two-photon absorption process, which involves the quasi-simultaneously absorption of two individual photons *via* a virtual state inside the bandgap of ZnO (Fig.23). This effect has been largely demonstrated in the case of ZnO microtubes[162], ZnO nanowires[163] and ZnO nanoparticles[164] but was

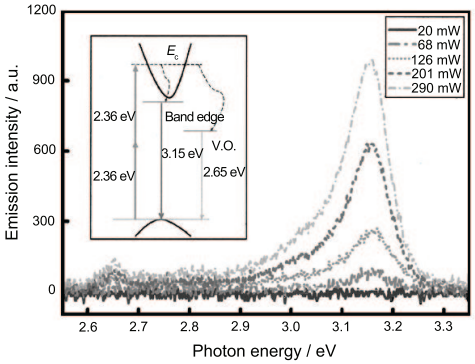

Fig.23 Two-photon-induced PL spectra excited by 527 nm nanosecond beam at different excitation powers, the inset is a schematic diagram of the electron transitions[162]

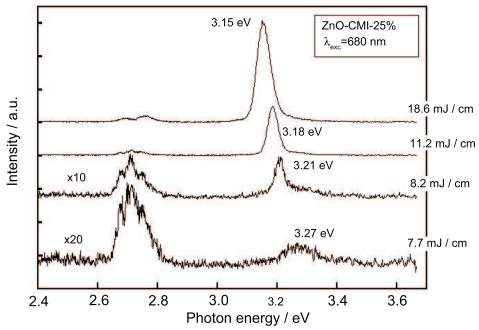

Fig.24 Emission spectra (λ=680 nm, E=1.82 eV) of sample ZnO/CMI-1 for various pumping intensities[136]

never studied in ZnO/SiO_2 nanocomposites.

To highlight such laser effect arising from one and two-photon absorption process, the ZnO-based mesoporous silicas nanocomposites prepared by the impregnation in concentrated $Zn(NO_3)_2$ aqueous solutions were submitted to a femtosecond excitation light provided by a mode-locked Ti: sapphire laser oscillator[136]. The incident wavelength was set at 340 and 680 nm for the one- and two-photon absorption experiments, respectively.

For excitation at 340 nm (3.65 eV photon energy), at low pumping intensities (2.2 mJ/cm^2), the emission spectrum of ZnO/SiO_2 nanocomposite is dominated by a broad band at 3.22 eV corresponding to the radiative recombination of excitons in ZnO. If the pumping intensity is slightly increased to 2.5 mJ/cm^2, the broad band becomes much narrower, meaning that laser action in ZnO-based nanocomposite is occurring. The mechanism of lasing is based on the light scattering within the mesoporous SiO_2 where active ZnO nanoparticles are introduced. The ZnO particles are well-dispersed into the mesopores of the silica network so that the amplification of the light is guaranteed by the loop formed by the light scattering, as explained previously. Interestingly, the laser effect in ZnO/SiO_2 nanocomposite was also demonstrated after a two-photon absorption process using an incident wavelength of 680 nm (1.82 eV photon energy) (Fig.24). When the pumping intensity is low (7.7 mJ/cm^2), a broad band at 3.27 eV is observed and represents the traditional excitonic emission of ZnO. Upon increasing slightly the pumping intensity (8.2 mJ/cm^2), a narrower peak is emerging and is attributed to stimulated emission produced by light scattering into ZnO/SiO_2 nanocomposite powders (Fig.25). Despite the fact that the incident photon energy (1.82 eV) is two times lower than the ZnO bandgap (3.37 eV), the observation of spontaneous and stimulated emissions indicates that electrons are effectively excited into the conduction band of ZnO. As a consequence, the excitation process involves the simultaneously absorption of two photons.

To the best of our knowledge, this is the unique report of one- and two-photon absorption resulting in laser action in ZnO/SiO_2 nanocomposites. This phenomenon is of significant importance since short-wavelength devices are required by industry to design new information storage materials. Regarding biological applications, the two-photon laser effect in ZnO/SiO_2 nanocomposites opens new ways to monitor biological objects with spatial resolution. Indeed, the emission of ZnO nanoparticles produced after IR excitation (680 nm) is coming only from the focal point of the incident laser beam contrary to UV excitation (340 nm), which induces emission produced by the whole excited volume. Assuming that ZnO nanoparticles can be grafted to biological objects, it is therefore possible to detect PL or lasing effect originating from very localized areas in samples.

4. ZnO inside Microporous Zeolites: Preparation and Optical Properties

Although ZnO nanoparticles introduced inside the channels of mesoporous silicas have shown remarkable optical properties, QSE and efficient laser action under one- and two-photon excitation process, it is still important to grow ZnO particles with a perfect control of their size in the nanometric range. Mesoporous silicas have appeared to be ideal hosts for such ZnO/SiO_2 nanocomposites but their pore size does not allow reaching dimensions smaller than 2.0 nm. Therefore, microporous zeolite materials with channels ranging from 0.5 to 2.0 nm have been used as matrices to introduce II-VI semiconducting nanoparticles, in particular CdS[165-169] and ZnO. In the following section, the preparation of ZnO nanoparticles inside the channels and cavities of microporous zeolitic materials will be reviewed.

One of the first reports of ZnO inside zeolites framework was published in 1997. Zinc acetate solutions were used to infiltrate Zn^{2+} inside the porous structure and then, sodium hydroxide was added to precipitate the ZnO nanoparticles inside faujasite and EMT-type zeolites[170]. In comparison to bulk ZnO, the absorption onset of ZnO/zeolite nanocomposites was blue-shifted, which was attributed, according to the authors, to the QSE from extremely small particles of ZnO. However after the growth of the ZnO nanoparticles inside zeolites, the crystalline structure appeared to be slightly modified[171]. Indeed, the ion-exchange of compensating zeolite cations (typically Na^+ and K^+) by Zn^{2+} ions results in small changes in the geometry and the symmetry of the structure, which can be observed by shifts of diffraction peaks in the XRD patterns and broadenings of signals in ^{27}Al and ^{29}Si NMR (nuclear magnetic resonance) spectra. When the size of ZnO nanoparticles is small were

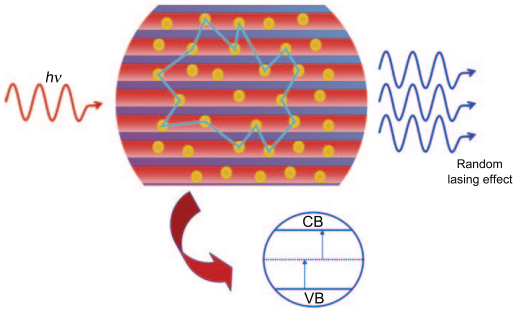

Fig.25 Schematic representation of random lasing effect of ZnO nanoparticles embedded in the hexagonally arranged cylindrical channels of highly ordered mesoporous silica CMI-1

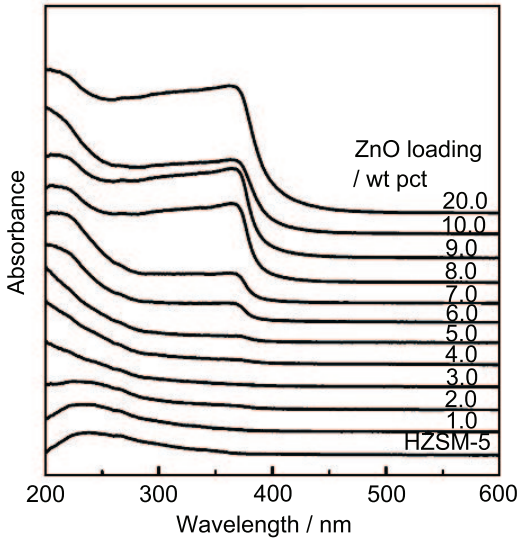

Fig.26 UV-visible absorption spectra of ZnO/HZSM-5 with different ZnO loadings. The spectrum of HZSM-5 was added for comparison[173]

enough to produce significant QSE, XRD patterns of ZnO/faujasite nanocomposites does not reveal any diffraction peaks associated with crystalline wurtzite ZnO[172].

ZnO nanoparticles also prepared inside the microporous structures of ZSM-5, FAU and Beta-type zeolites by the impregnation into aqueous zinc nitrate solutions followed by calcination at 550°C[173,174]. The authors showed the same trend, namely that small ZnO particles exhibiting QSE have no diffraction peak in the corresponding XRD pattern. In this study, different ZnO quantities were loaded inside the zeolites. At small ZnO loading, the absorption onset and the defect PL band were blue-shifted towards lower wavelengths because of the expected QSE. When the ZnO loading in ZSM-5 zeolite was increased, the QSE disappeared because the unidirectional channels and the silica-rich composition are unfavorable for the good dispersion of ZnO inside the network, and consequently, large ZnO particles are formed outside the micropores (Fig.26). In FAU zeolite, the observed QSE was still present at high ZnO loadings because the 3-dimensional pore system allows a good diffusion of Zn^{2+} ions and consequently, an efficient formation of extremely small ZnO particles (Fig.27).

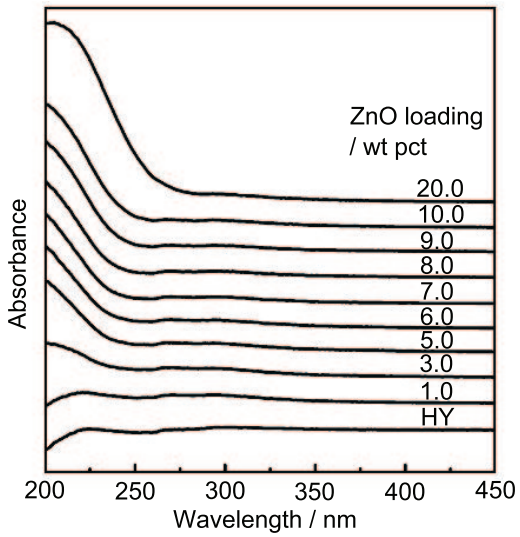

Fig.27 UV-visible absorption spectra of ZnO/HY with different ZnO loadings. The spectrum of HY was added for comparison[173]

The same conclusions were drawn for ZnO/FAU nanocomposites studied by our group with additional ^{27}Al and ^{29}Si NMR results[175,176]. The ZnO incorporation was performed by impregnating the FAU-type zeolite in $Zn(NO_3)_2$ solutions with various concentrations. No diffraction peak corresponding to crystalline ZnO was detected in the XRD patterns of ZnO/FAU nanocomposites until a very high ZnO loading (44 wt pct). However, slight shifts towards higher 2θ angles were observed in the XRD patterns of the parent FAU zeolite for nanocomposites with loadings ranging from 19 to 44 wt pct. This was attributed to the ion-exchange of monovalent Na^+ and K^+ ions for bivalent Zn^{2+} ions, which can play a role of the compensating cations in the negative-charged zeolite structure. Furthermore, the signals ascribed to Si atoms with 4 Al neighbors and to tetrahedrally coordinated Al in ^{29}Si and ^{27}Al NMR spectra, respectively, are significantly broadened in both cases, confirming the strong interaction created between Zn^{2+} and FAU zeolite. The optical properties of these nanocomposites have been studied under 6.4 eV excitation and have shown very interesting behavior (Fig.28). For samples with loadings in the range 1–12 wt pct, the PL spectra are identical to that of unloaded FAU zeolite. When the quantity of ZnO is increased up to 15 wt pct, a more intense and blue-shifted band appeared corresponding to the excitonic emission of ZnO nanoparticles grown inside the channels and cavities of FAU zeolite. For the sample with the highest loading (44 wt pct), an additional contribution at 3.2 eV can be detected in the PL spectrum. In conclusion, when the concentration of the $Zn(NO_3)_2$ solution is too low, the Zn^{2+} ions simply act as the counter-ions in the zeolite and no ZnO particles are formed upon calcination. A critical Zn precursor concentration has to be reached in order to grow ZnO particles exhibiting strong QSE due to their extremely small dimensions conferred by the limiting channels and cavities of FAU zeolite (Fig.29).

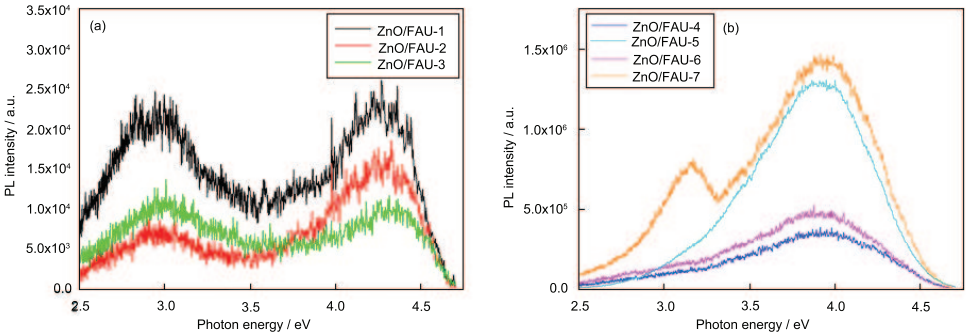

Fig.28 PL spectra of the ZnO/FAU nanocomposites with low ZnO loadings (a) and high ZnO loadings (b) (E_{exc}=6.4 eV)[176]

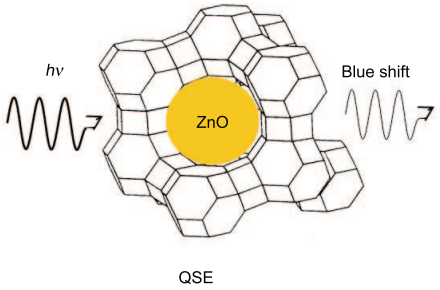

Fig.29 Scheme depicting the introduction of ZnO nanoparticles inside the channels and cavities of a FAU-type zeolite[175]

5. Conclusions

The state of the art in the preparation of ZnO/SiO_2 nanocomposites based on the introduction of ZnO nanoparticles inside the porosity of microporous and mesoporous silica materials has been largely reviewed. A particular attention was paid to the optical properties in order to highlight the quantum size effect (QSE) and the random lasing effect arising from extremely small ZnO nanoparticles confined inside the porous materials.

MCM-41 mesoporous materials have successfully been employed for the preparation of GaAs and InP-based nanocomposites and the expected QSE was observed. CdS was also introduced efficiently inside the mesopores of MCM-41 and SBA-15 silicas. Different loading methods have been used such as the preliminary surface modification of the silica materials and the formation of CdS nanoparticles inside reverse micelles.

A great number of studies have been devoted to the encapsulation of ZnO nanoparticles inside SiO_2 prepared by sol-gel method. Because of the heterogeneity of such systems, the blue-shift of the emission band of ZnO attributed to QSE was not systematically observed. Therefore, well-organised silica mesoporous materials have been used as hosts for the incorporation of ZnO particles. The first works were dedicated to the growth of ZnO inside silica materials whose internal surfaces have been modified with organic molecules able to complex Zn^{2+} cations in order to facilitate their diffusion inside the structure. UV-Vis measurements allowed the authors to confirm that ZnO nanoparticles have been grown inside the channels of MCM-41 materials.

Pure MCM-41 silicas without surface modification have also been used as hosts and have been impregnated in different zinc precursor solutions to give ZnO/MCM-41 nanocomposites with strong QSE revealed by UV-Vis or PL spectroscopy.

Recently, it has been demonstrated that the growth of extremely small particles of ZnO can be achieved in the mesoporosity of CMI-1 materials and that the excitonic emission of ZnO is blue-shifted towards higher energies due to QSE. In the same way, ZnS nanoparticles can be introduced in the channels of CMI-1 silicas.

Other loading methods, such as the spray-drying process and the utilization of reverse micelles systems, have been considered by many scientists to lead to ZnO/SiO_2 nanocomposites showing very strong QSE due to ZnO nanoparticles confined inside the structure of the silica matrix.

A special property of ZnO nanoparticles was highlighted. Indeed, in nanopowders media, it is possible to produce lasing effect coming from the multiple scattering of light on the active nanoparticles and the amplification of the light by the formation of loops inside the random media. To induce such effect, a femtosecond laser beam was focused on ZnO/CMI-1 nanocomposites and the intensity of the incident beam has been increased progressively. At low pumping intensity, the excitonic emission of ZnO has been observed. Upon increasing the pumping intensity above a threshold value, the excitonic emission turned to stimulated emission meaning that random lasing effect takes place. This effect has also been demonstrated for the first time for ZnO/CMI-1 nanocomposites after a two-photon excitation[177].

A complete survey of the ZnO incorporation by the impregnation method inside the microporous structure of zeolites was given. It was shown that silica-rich ZSM-5 zeolite with unidirectional channels was not an ideal matrix to grow small ZnO nanoparticles unlike FAU-type zeolite with 3-D channels and cavities which allowed the efficient growth of ZnO inside the zeolitic structure. By varying the concentration of the initial zinc precursor solution, our group has evidenced that no ZnO particles could be formed if the $Zn(NO_3)_2$ is too low. A critical Zn precursor concentration has to be reached in order to grow ZnO particles exhibiting strong QSE.

6. Outlooks

Future work has also to be realized regarding

the utilization of these optoelectronic nanocomposites in various optic and electronic devices. Indeed, the nanocomposites powders have to be immobilized on supports in order to guarantee their convenience and to give some directionality to their luminescence and lasing effect. Therefore, the next challenge will imply the preparation of ordered mesoporous silicas with channels perpendicular to the substrate and the incorporation of semiconductive nanoparticles inside the mesopores of the matrix by the loading methods, which have been reviewed in this paper. The aim of this approach is to design light-emitting devices with UV or blue-light emission which allow, for instance, to store more information on a given surface than IR-conventional information storage.

On the other hand, regarding biological applications, the two-photon absorption random lasing phenomenon opens new ways to monitor biological objects with spatial resolution. Indeed, the emission of ZnO nanoparticles produced after IR excitation is coming only from the focal point of the incident laser beam contrary to UV excitation, which induces emission produced by the whole excited volume. Assuming that ZnO nanoparticles can be grafted to biological objects, it is therefore possible to detect PL or lasing effect originating from very localised areas in the sample.

Acknowledgements

Claire Bouvy thanks the FNRS (Fonds National de la Recherche Scientifique, Belgium) for a FRIA doctoral fellowship and then a "Chargé de Recherches" fellowship. This work was realised in the frame of the Belgian Federal Government PAI-IUAP program (INANOMAT P6/17). The financial support from the University of Namur (FUNDP), "Aide institutionnelle aux collaborations internationales" is also acknowledged.

REFERENCES

[1] R.P.Feynman: *Eng. Sci.,* 1960, **23**, 22.
[2] L.E.Brus: *J. Chem. Phys.,* 1984, **80**, 4403.
[3] L.E.Brus: *J. Lum.,* 1984, **31-32**, 381.
[4] A.Henglein: *Chem. Rev.,* 1989, **89**, 1861.
[5] A.P.Alivisatos: *Science,* 1996, **271**, 933.
[6] S.Baskoutas and A.F.Terzis: *J. Appl. Phys.,* 2006, **99**, 013708.
[7] S.Baskoutas, A.F.Terzis and W.Schommers: *J. Comput. Theor. Nanosci.,* 2006, **3**, 1.
[8] E.Schrödinger: *Phys. Rev.,* 1926, **28**, 1049.
[9] D.J.Griffiths: *Introduction to Quantum Mechanics,* 2nd edn, Prentice Hall, 2004.
[10] A.I.Ekimov, A.L.Efros and A.A.Onushchenko: *Solid State Commun.,* 1985, **56**, 921.
[11] Y.Wang and N.Herron: *J. Phys. Chem.,* 1991, **95**, 525.
[12] L.T.Canham: *Appl. Phys. Lett.,* 1990, **57**, 1046.
[13] L.T.Canham: *Phys. Status Solidi B,* 1995, **190**, 9.
[14] P.F.Trwoga, A.J.Kenyon and C.W.Pitt: *J. Appl. Phys.,* 1998, **83**, 3789.
[15] J.P.Wolfe: *Phys. Today,* 1982, **March 46**.
[16] A.A.Guzelian, U.Banin, A.V.Kadavanich, X.Peng and A.P.Alivisatos: *Appl. Phys. Lett.,* 1996, **69**, 1432.
[17] U.Banin: *Nature,* 1999, **400**, 452.
[18] V.L.Colvin, M.C.Schlamp and A.P.Alivisatos: *Nature,* 1994, **370**, 354.
[19] M.G.Bawendi, W.L.Wilson, L.Rothberg, P.J.Carroll, T.M.Jedju, M.L.Steigerwald and L.E.Brus: *Phys. Rev. Lett.,* 1990, **65**, 1623.
[20] C.B.Murray, D.J.Norris and M.G.Bawendi: *J. Am. Chem. Soc.,* 1993, **115**, 8706.
[21] S.Gorer and G.Hodes: *J. Phys. Chem.,* 1994, **98**, 5338.
[22] X.Peng, L.Manna, W.Yang, J.Wickham, E.Scher, A.Kadavanich and A.P.Alivisatos: *Nature,* 2000, **404**, 59.
[23] D.S.King and R.M.Nix: *J. Catal.,* 1996, **160**, 76.
[24] F.Xu, Z.Y.Yuan, G.H.Du, T.Z.Ren, C.Bouvy, M.Halasa and B.L.Su: *Nanotechnology,* 2006, **17**, 588.
[25] F.Quaranta, A.Valentini, F.R.Rizzi and G.Casamassima: *J. Appl. Phys.,* 1993, **74**, 244.
[26] G.Agarwal and R.F.Speyer: *J. Electrochem. Soc.,* 1998, **145**, 2920.
[27] T.Wada, S.Kikuta, M.Kiba, K.Kiyozumi, T.Shimojo and M.Kakehi: *J. Cryst. Growth,* 1982, **59**, 363.
[28] C.Klingshirn, H.Kalt, R.Renner and F.Fidorra: *J. Cryst. Growth,* 1985, **72**, 304.
[29] G.H.Schoenmakers, D.Vanmaekelbergh and J.J.Kelly: *J. Phys. Chem. B,* 1996, **100**, 3215.
[30] B.D.Yao, H.Z.Shi, H.J.Bi and L.D.Zhang: *J. Phys. Condens. Mat.,* 2000, **12**, 6265.
[31] Y.C.Kong, D.P.Yu, B.Zhang, W.Fang and S.Q.Feng: *Appl. Phys. Lett.,* 2001, **78**, 407.
[32] J.Zhong, A.H.Kitai, P.Masher and W.Puff: *J. Electrochem. Soc.,* 1993, **140**, 3644.
[33] K.Keis, L.Vayssieres, S.E.Lindquist and A.Hagfeldt: *J. Electrochem. Soc.,* 2001, **148**, A149.
[34] D.R.Clarke: *J. Am. Ceram. Soc.,* 1999, **82**, 485.
[35] N.T.Hung, N.D.Quang and S.Bernik: *J. Mater. Res.,* 2001, **16**, 2817.
[36] Y.Shimizu, F.C.Lin, Y.Takao and M.Egashira: *J. Am. Ceram. Soc.,* 1998, **81**, 1633.
[37] R.Paneva and D.Gotchev: *Sensor. Actuat. A-Phys.,* 1999, **72**, 79.
[38] L.Gao, Q.Li and W.L.Luan: *J. Am. Ceram. Soc.,* 2002, **85**, 1016.
[39] K.Ip, G.T.Thaler, H.Yang, S.Y.Han, Y.Li, D.P.Norton, S.J.Pearton, S.Jang and F.Ren: *J. Cryst. Growth,* 2006, **287**, 149.
[40] C.Klingshirn: *Phys. Status Solidi. B,* 1975, **71**, 547.
[41] D.G.Thomas: *J. Phys. Chem. Solids,* 1960, **15**, 86.
[42] J.M.Hvam: *Solid State Commun.,* 1978, **26**, 987.
[43] C.Klingshirn, R.Hauschild, H.Priller, M.Decker, J.Zeller and H.Kalt: *Superlattice. Microst.,* 2005, **38**, 209.
[44] D.M.Bagnall, Y.F.Chen, Z.Zhu and T.Yao: *Appl. Phys. Lett.,* 1998, **73**, 1038.
[45] D.M.Bagnall, Y.F.Chen, M.Y.Shen, Z.Zhu, T.Goto and T.Yao: *J. Cryst. Growth,* 1998, **184/185**, 605.
[46] I.Ozerov, D.Nelson, A.V.Bulgakov, W.Marine and M.Sentis: *Appl. Surf. Sci.,* 2003, **212-213**, 349.
[47] I.Ozerov, M.Arab, V.I.Safarov, W.Marine, S.Giorgio, M.Sentis and L.Nanai: *Appl. Surf. Sci.,* 2004, **226**, 242.
[48] H.J.Egelhaaf and D.Oelkrug: *J. Cryst. Growth,* 1996, **161**, 190.
[49] K.Vanheusden, W.L.Warren, C.H.Seager, D.R.Tallant, J.A.Voigt and B.E.Gnade: *J. Appl. Phys.,* 1996, **79**, 7983.
[50] E.G.Bylander: *J. Appl. Phys.,* 1978, **49**, 1188.
[51] A.Janotti and C.G.Vandewalle: *Appl. Phys. Lett.,* 2005, **87**, 122102.
[52] G.Beni and T.M.Rice: *Phys. Rev. B,* 1978, **18**, 768.
[53] P.Vashishita and R.K.Kalia: *Phys. Rev. B,* 1982, **25**, 6492.
[54] Z.L.Wang: *Mater. Today,* 2004, **7**, 26.
[55] X.Wang, J.Song and Z.L.Wang: *Chem. Phys. Lett.,* 2006, **424**, 86.

[56] X.Fang and L.Zhang: *J. Mater. Sci. Technol.,* 2006, **22**, 1.
[57] C.Pacholski, A.Kornowski and H.Weller: *Angew. Chem. Int. Edit.,* 2002, **41**, 118.
[58] J.C.Johnson, H.Yan, R.D.Schaller, L.H.Haber, R.J.Saykally and P.Yang: *J. Phys. Chem. B,* 2001, **105**, 11387.
[59] F.Xu, G.H.Du, M.Halasa and B.L.Su: *Chem. Phys. Lett.,* 2006, **426**, 129.
[60] Z.W.Pan, Z.R.Dai and Z.L.Wang: *Science,* 2001, **291**, 1947.
[61] J.J.Wu, S.C.Liu, C.T.Wu, K.H.Chen and L.C.Chen: *Appl. Phys. Lett.,* 2002, **81**, 1312.
[62] P.X.Gao, Y.Ding, W.Mai, W.L.Hugues, C.Lao and Z.M.Wang: *Science,* 2005, **309**, 1700.
[63] F.Xu, Z.Y.Yuan, G.H.Du, M.Halasa and B.L.Su: *Appl. Phys. A,* 2007, **86**, 181.
[64] F.Xu, Z.Y.Yuan, G.H.Du, T.Z.Ren, C.Volcke, P.Thiry and B.L.Su: *J. Non-Cryst. Growth,* 2006, **352**, 2569.
[65] J.Lao, J.G.Wen and Z.F.Ren: *Nano Lett.,* 2002, **2**, 1287.
[66] F.Xu, P.Zhang, A.Navrotsky, Z.Y.Yuan, T.Z.Ren, M.Halasa and B.L.Su: *Chem. Mater.,* 2007, **19**, 5680.
[67] Z.L.Wang: *J. Phys.*, 2006, **26**, 1.
[68] H.J.Ko, Y.Chen, S.K.Hong and T.Yao: *J. Cryst. Growth,* 2000, **209**, 816.
[69] A.Ohtomo, M.Kawasaki, Y.Sakurai, Y.Yoshida, H.Koinuma, P.Yu, Z.K.Tang, G.K.L.Wong and Y.Segawa: *Mater. Sci. Eng. B,* 1998, **54**, 24.
[70] Y.W.Heo, V.Varadarajan, M.Kaufman, K.Kim and D.P.Norton: *Appl. Phys. Lett.,* 2002, **81**, 3046.
[71] A.Yamamoto, T.Kido, T.Goto, Y.F.Chen and T.Yao: *Appl. Phys. Lett.,* 1999, **75**, 469.
[72] J.F.Muth, R.M.Kolbas, A.K.Sharma, S.Oktyabrsky and J.Narayan: *J. Appl. Phys.,* 1999, **85**, 7884.
[73] Y.Zhang, R.E.Russo and S.S.Mao: *Appl. Phys. Lett.,* 2005, **87**, 133115.
[74] H.Usui, Y.Shimizu, T.Sasaki and N.Koshizaki: *J. Phys. Chem. B,* 2005, **109**, 120.
[75] A.Said, L.Sajti, S.Giorgio and W.Marine: *J. Phys.,* 2007, **59**, 259.
[76] C.L.Sajti, S.Giorgio, V.Khodorkovsky and W.Marine: *Appl. Phys. A,* 2007, **89**, 315.
[77] C.L.Sajti, S.Giorgio, V.Khodorkovsky and W.Marine: *Appl. Surf. Sci.,* 2007, **253**, 8111.
[78] T.Gruber, C.Kirchner, K.Thonke, R.Sauer and A.Waag: *Phys. Status Solidi A,* 2002, **192**, 166.
[79] Z.X.Fu, B.X.Lin and J.Zu: *Thin Solid Films,* 2002, **402**, 302.
[80] W.I.Park, D.H.Kim, S.W.Jung and G.C.Yi: *Appl. Phys. Lett.,* 2002, **80**, 4232.
[81] C.Munuera, J.Zuniga-Perez, J.F.Rommeluere, V.Sallet, R.Triboulet, F.Soria, V.Munoz-Sanjose and C.Ocal: *J. Cryst. Growth,* 2004, **264**, 70.
[82] Y.Li, G.W.Meng, L.D.Zhang and F.Philipp: *Appl. Phys. Lett.,* 2000, **76**, 2011.
[83] M.J.Zheng, L.D.Zhang, G.H.Li and W.Z.Shen: *Chem. Phys. Lett.,* 2002, **363**, 123.
[84] L.Spanhel and M.A.Anderson: *J. Am. Chem. Soc.,* 1991, **113**, 2826.
[85] L.Znaidi, G.J.A.A.Soler-Illia, S.Benyahia, C.Sanchez and A.V.Kanaev: *Thin Solid Films,* 2003, **428**, 257.
[86] E.Matijevic: *Langmuir,* 1986, **2**, 12.
[87] E.A.Meulekamp: *J. Phys. Chem. B,* 1998, **102**, 5566.
[88] J.M.Wang and L.Gao: *Solid State Commun.,* 2004, **132**, 269.
[89] Y.D.Wang, K.Y.Zang, S.J.Chua and C.G.Fonstad: *Appl. Phys. Lett.,* 2006, **89**, 263116.
[90] Y.Tong, Y.Liu, L.Dong, D.Zhao, J.Zhang, Y.Lu, D.Shen and X.Fan: *J. Phys. Chem. B,* 2006, **110**, 20263.
[91] J.Zhang, B.Han, Z.Hou, Z.Lin, J.He and T.Jiang: *Langmuir,* 2003, **19**, 7616.
[92] E.M.Wong, P.G.Hoertz, C.J.Liang, B.M.Shi, G.J.Meyer and P.C.Searson: *Langmuir,* 2001, **17**, 8362.
[93] M.Oner, J.Norwig, W.H.Meyer and G.Wegner: *Chem. Mater.,* 1998, **10**, 460.
[94] L.Guo, S.Yang, C.Yang, P.Yu, J.Wang, W.Ge and G.K.L.Wong: *Chem. Mater.,* 2000, **12**, 2268.
[95] H.M.Xiong, X.Zhao and J.S.Chen: *J. Phys. Chem. B,* 2001, **105**, 10169.
[96] W.Feng, H.Tao, Y.Liu and Y.Liu: *J. Mater. Sci. Technol.,* 2006, **22**, 230.
[97] J.Weitkam: *Solid State Ionics,* 2000, **131**, 175.
[98] J.S.Beck, J.C.Vartuli, W.J.Roth, M.E.Leonowicz, C.T.Kresge, K.D.Schmitt, C.T.W.Chu, D.H.Olson, E.W.Sheppard, S.B.McCullen, J.B.Higgins and J.L.Schlenker: *J. Am. Chem. Soc.,* 1992, **114**, 10834.
[99] C.T.Kresge, M.E.Leonowicz, W.J.Roth, J.C.Vartuli and J.S.Beck: *Nature,* 1992, **359**, 710.
[100] K.Moller and T.Bein: *Chem. Mater.,* 1998, **10**, 2950.
[101] J.Zhang, Z.Luz and D.Goldfarb: *J. Phys. Chem. B,* 1997, **101**, 7087.
[102] A.Galarneau, F.Di Renzo, F.Fajula, L.Mollo, B.Fubini and M.F.Ottaviani: *J. Colloid Interf. Sci.,* 1998, **201**, 105.
[103] J.Zhang, Z.Luz, H.Zimmerman and D.Goldfarb: *J. Phys. Chem. B,* 2000, **104**, 279.
[104] J.Zhang and D.Goldfarb: *Micropor. Mesopor. Mat.,* 2001, **48**, 143.
[105] Y.Wan and D.Zhao: *Chem. Rev.,* 2007, **107**, 2821.
[106] D.Zhao, J.Feng, Q.Huo, N.Melosh, G.H.Fredrickson, B.F.Chmelka and G.D.Stucky: *Science,* 1998, **279**, 548.
[107] S.A.Bagshaw, E.Prouzet and T.J.Pinnavaia: *Science,* 1995, **269**, 1242.
[108] J.L.Blin, A.Leonard and B.L.Su: *Chem. Mater.,* 2001, **13**, 3542.
[109] A.Corma: *Chem. Rev.,* 1997, **97**, 2373.
[110] B.J.Scott, G.Wirnsberger and G.D.Stucky: *Chem. Mater.,* 2001, **13**, 3140.
[111] V.I.Srdanov, I.Alxneit, G.D.Stucky, C.M.Reaves and S.P.Den Baars: *J. Phys. Chem. B,* 1998, **102**, 3341.
[112] J.R.Agger, M.W.Anderson, M.E.Pemble, O.Terasaki and Y.Nozue: *J. Phys. Chem. B,* 1998, **102**, 3345.
[113] H.Wellmann, J.Rathousky, M.Wark, A.Zukal and G.Schulz-Ekloff: *Micropor. Mesopor. Mat.,* 2001, **44-45**, 419.
[114] F.Gao, Q.Lu and D.Zhao: *Chem. Phys. Lett.,* 2002, **360**, 585.
[115] W.Xu, Y.Liao and D.L.Akins: *J. Phys. Chem. B,* 2002, **106**, 11127.
[116] S.Wang, D.G.Choi and S.M.Yang: *Adv. Mater.,* 2002, **14**, 1311.
[117] T.Hirai, H.Okubo and I.Komasawa: *J. Phys. Chem. B,* 1999, **103**, 4228.
[118] C.Bouvy, F.Piret, W.Marine and B.L.Su: *Chem. Phys. Lett.,* 2007, **433**, 350.
[119] L.Chen, P.J.Klar, W.Heimbrodt, F.Brieler, M.Froba, H.A.Krug von Nidda, T.Kurz and A.Loidl: *J. Appl. Phys.,* 2003, **93**, 1326.
[120] F.J.Brieler, P.Grundmann, M.Froba, L.Chen, P.J.Klar, W.Heimbrodt, H.A.Krug von Nidda, T.Kurz and A.Loidl: *J. Am. Chem. Soc.,* 2004, **126**, 797.
[121] C.Cannas, M.Casu, A.Lai, A.Musinu and G.Piccaluga: *J. Mater. Chem.,* 1999, **9**, 1765.
[122] *Powder Diffraction File,* Card No.19-1479 (International Center for Diffraction Data, Swarthmore, PA)
[123] L.Armelao, M.Fabrizio, S.Gialanella and F.Zordan: *Thin Solid Films,* 2001, **394**, 90.
[124] S.Chakrabarti, D.Ganguli and S.Chaudhuri: *J. Phys. D: Appl. Phys.,* 2003, **36**, 146.

[125] S.Chakrabarti, D.Das, D.Ganguli and S.Chaudhuri: *Thin Solid Films,* 2003, **441**, 228.
[126] H.He, Y.Wang and Y.Zou: *J. Phys. D: Appl. Phys.,* 2003, **36**, 2972.
[127] S.Zhao, Z.Ji, Y.Yang, D.Huo and Y.Lv: *Mater. Lett.,* 2007, **61**, 2547.
[128] W.H.Zhang, J.L.Shi, L.Z.Wang and D.S.Yan: *Chem. Mater.,* 2000, **12**, 1408.
[129] H.G.Chen, J.L.Shi, H.R.Chen, J.N.Yan, Y.S.Li, Z.L.Hua, Y.Yang and D.S.Yan: *Opt. Mater.,* 2004, **25**, 79.
[130] C.Cannas, M.Mainas, A.Musinu and G.Piccaluga: *Compos. Sci. Technol.,* 2003, **63**, 1187.
[131] W.Zeng, Z.Wang, X.F.Qian, J.Yin and Z.K.Zhu: *Mater. Res. Bull.,* 2006, **41**, 1155.
[132] Y.Xiong, L.Z.Zhang, G.Q.Tang, G.L.Zhang and W.J.Chen: *J. Lum.,* 2004, **110**, 17.
[133] G.Q.Tang, Y.Xiong, L.Z.Zhang and G.L.Zhang: *Chem. Phys. Lett.,* 2004, **395**, 97.
[134] L.I.Burova, D.I.Petukhov, A.A.Eliseev, A.V.Lukashin and Y.D.Tretyakov: *Superlattice. Microst.,* 2006, **39**, 257.
[135] C.Bouvy, W.Marine, R.Sporken and B.L.Su: *Chem. Phys. Lett.,* 2006, **420**, 225.
[136] C.Bouvy, E.Chelnokov, W.Marine, R.Sporken and B.L.Su: *Appl. Phys. A,* 2007, **88**, 105.
[137] F.Piret, C.Bouvy, W.Marine and B.L.Su: *Chem. Phys. Lett.,* 2007, **441**, 83.
[138] A.Mikrajuddin, F.Iskandar, K.Okuyama and F.G.Shi: *J. Appl. Phys.,* 2001, **89**, 6431.
[139] A.Mikrajuddin, S.Shibamoto and K.Okuyama: *Opt. Mater.,* 2004, **26**, 95.
[140] F.Gao, S.P.Naik, Y.Sasaki and T.Okubo: *Thin Solid Films,* 2006, **495**, 68.
[141] F.Gao, N.Chino, S.P.Naik, Y.Sasaki and T.Okubo: *Mater. Lett.,* 2007, **61**, 3179.
[142] R.Moleski, E.Leontidis and F.Krumeich: *J. Colloid Interface Sci.,* 2006, **302**, 246.
[143] C.Bouvy, W.Marine and B.L.Su: *Chem. Phys. Lett.,* 2007, **438**, 67.
[144] D.Wiersma: *Nature,* 2000, **406**, 132.
[145] D.Wiersma and S.Cavalieri: *Nature,* 2001, **414**, 708.
[146] H.Cao, Y.G.Zhao, S.T.Ho, E.W.Seelig, Q.H.Wang and R.P.H.Chang: *Phys. Rev. Lett.,* 1999, **82**, 2278.
[147] H.Cao, J.Y.Xu, E.W.Seelig and R.P.H.Chang: *Appl. Phys. Lett.,* 2000, **76**, 2997.
[148] H.Cao, J.Y.Xu, S.H.Chang and S.T.Ho: *Phys. Rev. E,* 2000, **61**, 1985.
[149] H.Cao: *Waves Random Media,* 2003, **13**, R1.
[150] R.K.Thareja and A.Mitra: *Appl. Phys. B,* 2000, **71**, 181.
[151] J.C.Johnson, H.Yan, P.Yang and R.J.Saykally: *J. Phys. Chem. B,* 2003, **107**, 8816.
[152] V.S.Letokhov: *Sov. Phys. JETP,* 1968, **26**, 835.
[153] C.Klingshirn: *J. Cryst. Growth,* 1992, **117**, 753.
[154] R.Cingolani and K.Ploog: *Adv. Phys.,* 1991, **40**, 535.
[155] D.C.Reynolds, D.C.Look and B.Jogai: *Solid State Commun.,* 1996, **99**, 873.
[156] D.M.Bagnall, Y.F.Chen, Z.Zhu, T.Yao, S.Koyama, M.Y.Shen and T.Goto: *Appl. Phys. Lett.,* 1997, **70**, 2230.
[157] P.Zu, Z.K.Tang, G.K.L.Wong, M.Kawasaki, A.Ohtomo, H.Koinuma and Y.Segawa: *Solid State Commun.,* 1997, **103**, 459.
[158] Z.K.Tang, G.K.L.Wong, P.Yu, M.Kawasaki, A.Ohtomo, H.Koinuma and Y.Segawa: *Appl. Phys. Lett.,* 1998, **72**, 3270.
[159] P.Yu, Z.K.Tang, G.K.L.Wong, M.Kawasaki, A.Ohtomo, H.Koinuma and Y.Segawa: *J. Cryst. Growth,* 1998, **184/185**, 601.
[160] M.Kawasaki, A.Ohtomo, I.Ohkubo, H.Koinuma, Z.K.Tang, P.Yu, G.K.L.Wong, B.P.Zhang and Y.Segawa: *Mater. Sci. Eng. B,* 1998, **56**, 239.
[161] Z.K.Tang, M.Kawasaki, A.Ohtomo, H.Koinuma and Y.Segawa: *J. Cryst. Growth,* 2006, **287**, 169.
[162] C.F.Zhang, Z.W.Dong, G.J.You, S.X.Qian, H.Deng, H.Gao, L.P.Yang and Y.Li: *Appl. Phys. Lett.,* 2005, **87**, 051920.
[163] C.F.Zhang, Z.W.Dong, G.J.You, R.Y.Zhu, S.X.Qian, H.Deng, H.Cheng and J.C.Wang: *Appl. Phys. Lett.,* 2006, **89**, 042117.
[164] E.V.Chelnokov, N.Bityurin, I.Ozerov and W.Marine: *Appl. Phys. Lett.,* 2006, **89**, 171119.
[165] Y.Wang and N.Herron: *J. Phys. Chem.,* 1988, **92**, 4988.
[166] W.Chen, Y.Xu, Z.Lin, Z.Wang and L.Lin: *Solid State Commun.,* 1998, **105**, 129.
[167] H.Villavicencio-Garcia, M.Hernandez-Velez, O.Sanchez-Garrido, J.M.Martinez-Duart and J.Jimenez: *Solid-State Electron.,* 1999, **43,** 1171.
[168] R.J.Martin-Palma, M.Hernandez-Velez, I.Diaz, H.Villavicencio-Garcia, M.M.Garcia-Poza, J.M.Martinez-Duart and J.Perez-Pariente: *Mater. Sci. Eng. C,* 2001, **15,** 163.
[169] F.Iacomi: *Surf. Sci.,* 2003, **532-535,** 816.
[170] M.Wark, H.Kessler and G.Schulz-Ekloff: *Microporous Mater.,* 1997, **8,** 241.
[171] L.Khouchaf, M.H.Tuilier, M.Wark, M.Soulard and H.Kessler: *Micropor. Mesopor. Mat.,* 1998, **20,** 27.
[172] F.Meneau, G.Sankar, N.Morgante, S.Cristol, C.R.A.Catlow, J.M.Thomas and G.N.Greaves: *Nucl. Instrum. Meth. B,* 2003, **199,** 499.
[173] J.Chen, Z.Feng, P.Ying and C.Li: *J. Phys. Chem. B,* 2004, **108,** 12669.
[174] J.Shi, J.Chen, Z.Feng, T.Chen, X.Wang, P.Ying and C.Li: *J. Phys. Chem. B,* 2006, **110,** 25612.
[175] C.Bouvy, W.Marine, R.Sporken and B.L.Su: *Chem. Phys. Lett.,* 2006, **428,** 312.
[176] C.Bouvy, W.Marine, R.Sporken and B.L.Su: *Colloid. Surface A,* 2007, **300,** 145.
[177] C.Bouvy, E.Chelnokov, R.Zhao, W.Marine, R.Sporken and B.L.Su: *Nanotechnology,* 2008, **19,** 105710.